

## VU Research Portal

### Optic axis determination accuracy for fiber-based polarization-sensitive optical cohernece tomography

Park, B. H.; Pierce, M. C.; Cense, B.; de Boer, J.F.

***published in***

Optics Letters  
2005

***DOI (link to publisher)***

[10.1364/OL.30.002587](https://doi.org/10.1364/OL.30.002587)

***document version***

Publisher's PDF, also known as Version of record

[Link to publication in VU Research Portal](#)

***citation for published version (APA)***

Park, B. H., Pierce, M. C., Cense, B., & de Boer, J. F. (2005). Optic axis determination accuracy for fiber-based polarization-sensitive optical cohernece tomography. *Optics Letters*, 30(19), 2587-2589.  
<https://doi.org/10.1364/OL.30.002587>

**General rights**

Copyright and moral rights for the publications made accessible in the public portal are retained by the authors and/or other copyright owners and it is a condition of accessing publications that users recognise and abide by the legal requirements associated with these rights.

- Users may download and print one copy of any publication from the public portal for the purpose of private study or research.
- You may not further distribute the material or use it for any profit-making activity or commercial gain
- You may freely distribute the URL identifying the publication in the public portal ?

**Take down policy**

If you believe that this document breaches copyright please contact us providing details, and we will remove access to the work immediately and investigate your claim.

**E-mail address:**

[vuresearchportal.ub@vu.nl](mailto:vuresearchportal.ub@vu.nl)

# Optic axis determination accuracy for fiber-based polarization-sensitive optical coherence tomography

B. Hyle Park, Mark C. Pierce, Barry Cense, and Johannes F. de Boer

Wellman Center for Photomedicine, Massachusetts General Hospital, Harvard Medical School, 50 Blossom Street, BAR 7, Boston, Massachusetts 02114

Received March 11, 2005; revised manuscript received June 3, 2005; accepted June 17, 2005

We present a generalized analysis of fiber-based polarization-sensitive optical coherence tomography with an emphasis on determination of sample optic axis orientation. The polarization properties of a fiber-based system can cause an overall rotation in a Poincaré sphere representation such that the plane of possible measured sample optic axes for linear birefringence and diattenuation no longer lies in the QU-plane. The optic axis orientation can be recovered as an angle on this rotated plane, subject to an offset and overall indeterminacy in sign such that only the magnitude, but not the direction, of a change in orientation can be determined. We discuss the accuracy of optic axis determination due to a fundamental limit on the accuracy with which a polarization state can be determined as a function of signal-to-noise ratio. © 2005 Optical Society of America

OCIS codes: 230.5440, 060.2340, 200.4860, 170.3880, 260.5430.

Polarization-sensitive optical coherence tomography (PS-OCT) is a noninvasive imaging technique capable of determining sample polarization properties.<sup>1–7</sup> These properties, including birefringence, diattenuation, and optic axis orientation, can be determined directly by studying the depth evolution of Stokes parameters<sup>1–4,6,8,9</sup> or indirectly by using the changing reflected polarization states to first determine Jones or Mueller matrices.<sup>5,10–14</sup> While the amounts of sample birefringence<sup>15–17</sup> and diattenuation<sup>14</sup> have been verified for fiber-based systems, obtaining the sample optic axis orientation is more complicated<sup>8,9,13,14,17,18</sup> and can be misinterpreted.<sup>19</sup> In this paper, we examine the relative sample optic axis orientation for a generalized fiber-based PS-OCT system and identify inherent ambiguities in offset and direction. Further, we discuss the accuracy of optic axis determination due to a fundamental limit on the accuracy with which a polarization state can be determined as a function of signal-to-noise ratio (SNR).

In general terms, a PS-OCT system sends polarized light from a broadband source into the sample and reference arms of an interferometer, and reflected light from both arms is recombined and detected. Define  $\mathbf{J}_{\text{in}}$  as the Jones matrix representing the optical path from the polarized light source to the sample surface,  $\mathbf{J}_{\text{out}}$  as that going from the sample surface to the detectors, and  $\mathbf{J}_S$  as the round-trip Jones matrix for light propagation through a sample.<sup>14</sup> This nomenclature can be applied to all PS-OCT systems, ranging from bulk-optic systems<sup>1–6</sup> to those with fibers placed such that they are traversed in a round-trip manner,<sup>13</sup> to time-domain<sup>8,20</sup> and spectral-domain<sup>21</sup> PS-OCT systems with unrestricted use of optical fiber and nondiattenuating fiber components, and even for retinal systems,<sup>22</sup> where the polarization effects of the cornea can be included in  $\mathbf{J}_{\text{in}}$  and  $\mathbf{J}_{\text{out}}$ . The electric field of light reflected from the sample surface,  $\mathbf{E}$ , can be expressed as

$\mathbf{E} = \exp(i\psi)\mathbf{J}_{\text{out}}\mathbf{J}_{\text{in}}\mathbf{E}_{\text{source}}$ , where  $\psi$  represents a common phase and  $\mathbf{E}_{\text{source}}$  represents the electrical field of light coming from the polarized source. Likewise, the electrical field of light reflected from some depth within the tissue may be described by  $\mathbf{E}' = \exp(i\psi')\mathbf{J}_{\text{out}}\mathbf{J}_S\mathbf{J}_{\text{in}}\mathbf{E}_{\text{source}}$ . These two measurable polarization states can be related to each other such that  $\mathbf{E}' = \exp[i(\psi' - \psi)]\mathbf{J}_T\mathbf{E}$ , where  $\mathbf{J}_T = \mathbf{J}_{\text{out}}\mathbf{J}_S\mathbf{J}_{\text{out}}^{-1}$ .

If the optical system represented by  $\mathbf{J}_{\text{out}}$  is nondiattenuating,  $\mathbf{J}_{\text{out}}$  can be treated as a unitary matrix with unit determinant after separating out a common attenuation factor.  $\mathbf{J}_S$  can be decomposed into a diagonal matrix  $\mathbf{J}_C$ , containing complete information regarding the amount of sample diattenuation and phase retardation, surrounded by unitary matrices  $\mathbf{J}_A$  with unit determinant that define the sample optic axis. We can reform  $\mathbf{J}_T$  such that  $\mathbf{J}_T = \mathbf{J}_{\text{out}}\mathbf{J}_S\mathbf{J}_{\text{out}}^{-1} = \mathbf{J}_{\text{out}}(\mathbf{J}_A\mathbf{J}_C\mathbf{J}_A^{-1})\mathbf{J}_{\text{out}}^{-1} = \mathbf{J}_U\mathbf{J}_C\mathbf{J}_U^{-1}$ , where  $\mathbf{J}_U = \mathbf{J}_{\text{out}}\mathbf{J}_A$ . Since unitary matrices with unit determinant form the special unitary group  $\text{SU}(2)$ ,<sup>23</sup>  $\mathbf{J}_U$  must also be a unitary matrix with unit determinant by closure. All members of  $\text{SU}(2)$  can be mapped to rotations in  $\text{SO}(3)$ , and so  $\mathbf{J}_{\text{out}}$ ,  $\mathbf{J}_A$ , and  $\mathbf{J}_U$  all represent rotations in a Poincaré sphere representation. This means that  $\mathbf{J}_C$ ,  $\mathbf{J}_S$ , and  $\mathbf{J}_T$  are related by unitary transforms and are equivalent except for their respective coordinate systems. Therefore, the amount of phase retardation and diattenuation in  $\mathbf{J}_C$ ,  $\mathbf{J}_S$ , and  $\mathbf{J}_T$  is the same. The three matrices differ only in their eigenvectors, and their optic axis equivalents, in a well-defined manner dictated by  $\mathbf{J}_{\text{out}}$ . In other words, the optic axis of  $\mathbf{J}_T$  is the product of the sample optic axis defined by  $\mathbf{J}_A$  and the fiber transformations represented by  $\mathbf{J}_{\text{out}}$ .

Due to the round-trip nature of detected light propagation in tissue, the circular components of birefringence and diattenuation in the sample cancel. Only the linear components of these properties can be measured using PS-OCT. In mathematical terms, the optic axes of  $\mathbf{J}_S$ , defined by its eigenvectors, can

represent only linear birefringence and diattenuation; the V-component (describing circular polarization effects) of the equivalent Stokes vector must equal zero. Therefore, all possible optic axes for  $\mathbf{J}_S$  lie on the QU-plane of a Poincaré sphere. Since  $\mathbf{J}_T$  and  $\mathbf{J}_S$  differ only by an overall rotation of their coordinate systems, the plane of all possible optic axes for  $\mathbf{J}_T$  can be rotated off the QU-plane to some arbitrary plane passing through the origin. The optic axes of  $\mathbf{J}_T$  can then have circular components that are entirely due to rotations of the coordinate system arising from system fiber. To verify this analysis, PS-OCT images were taken of a chicken muscle sample, its surface oriented orthogonal to the incident beam, and rotated in  $40^\circ$  increments to span a full  $360^\circ$ . Details of the fiber-based PS-OCT system, capable of imaging at 2048 depth scans/s, were presented by Pierce *et al.*<sup>20</sup> It should be noted that the sample itself was rotated and that the fibers in the system were left untouched. Two different analysis methods, a vector-based method<sup>8,9</sup> and a Jones-matrix-based method,<sup>14</sup> were used to analyze the data, providing nearly identical results. The resulting optic axes, along with a plane determined by least-squares fitting, are shown in the inset of Fig. 1. The rotation away from the QU-plane is evident, as is the coplanarity of the calculated optic axes.

One method of determining optic axis orientation is to simply determine the orientation as an angle on this tilted plane, as shown in Fig. 1. The resulting orientations, relative to that at  $0^\circ$ , are plotted as a function of the set orientation, and show that the relative optic axis orientation can be recovered accurately. A second method is to rotate the calculated plane of optic axes back down onto the QU-plane of the Poincaré sphere. The change in coordinate system due to optical fibers in the system can be decomposed into two parts: a rotation within the plane of possible measured optic axes and a tilting of the plane about some arbitrary axis in the QU-plane. The rotation within the plane causes an overall offset in the calculated orientation that has been discussed in previous publications<sup>13,18,24</sup> and implies that only

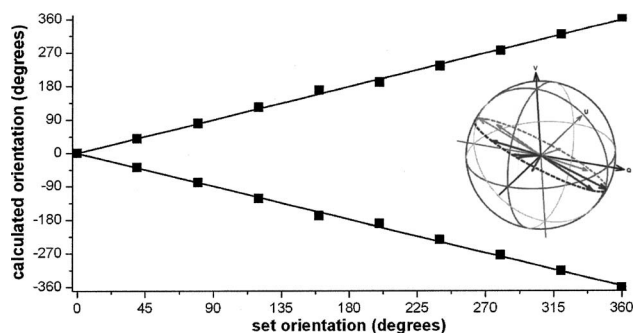


Fig. 1. Calculated optic axis orientation as a function of set orientation relative to  $0^\circ$  (squares, measured orientation; lines, linear fit to the data). As a result of the  $\pi$ -ambiguity (see text) the measured orientation can have both a positive and a negative slope with equal likelihood. Inset, Poincaré sphere representation of the calculated optic axes (arrows) for various set orientations of the tissue sample optic axis. The plane (dashed circle) in which these optic axes lie was determined by least-squares fitting.

relative orientation angles, not absolute angles, can be determined from a fiber-based PS-OCT system. The tilting of the plane leads to what can be termed a  $\pi$ -ambiguity, or an indeterminacy in the sign of the orientation angle.

One proposed method to compensate for this tilting uses the reflection from the surface of a sample to determine the rotation needed to tilt the plane back onto the QU-plane by solving  $\mathbf{E} = \exp(i\psi)\mathbf{J}_{in}^T\mathbf{J}_{in}\mathbf{E}_{source}$ , where  $\mathbf{J}_{in}$  represents the sample-arm fiber only.<sup>13</sup> Four possible solutions to  $\mathbf{J}_{in}$  can be found that map to two unique rotations in SO(3) corresponding to common phase factors  $\psi$  differing by  $\pi$ . This  $\pi$ -ambiguity is present in all fiber-based PS-OCT systems. In geometrical terms, this is the equivalent of the fact that there are two ways to rotate the plane of measured optic axes onto the QU-plane of the Poincaré sphere (face-up and face-down). This results in an ambiguity in the sign of the orientation angle. In other words, as the set optic axis orientation of a sample rotates in one direction, the measured optic axis orientation, depending on the correction chosen, could move in either direction. Thus, the sign of the orientation angle cannot be determined explicitly, only the absolute value, or magnitude, of change from one location to the next. The slope of Fig. 1, relating the calculated orientation to the set orientation for a set of data where the same correction could be used throughout, could be positive or negative with equal validity. This  $\pi$ -ambiguity is inherent in all fiber-based PS-OCT systems and implies that, although the relative optic axis within an image can be determined, the direction of change in optic axis orientation cannot be compared from image to image absolutely without *a priori* knowledge.

Since calculation of any sample polarization properties is dependent on determination of the polarization state of light measured with PS-OCT, the accuracy of these polarization properties is highly dependent on the accuracy of polarization state determination. One such fundamental limitation arises from the SNR of a measurement.<sup>21,25</sup> To quantify this effect, 1024 consecutive depth profiles at a single point on a glass slide were obtained at different SNRs using a variable neutral density filter in the sample arm of a spectral-domain PS-OCT system.<sup>21</sup> The polarization state reflected from the surface of the slide was determined, and the average angular deviation of these polarization states from their mean, as illustrated in the inset of Fig. 2, was calculated. The resulting data, plotted as a function of SNR in Fig. 2, demonstrate a decreasing average angular standard deviation with increasing SNR. The theoretical curve was generated based on a simple additive noise model. The standard deviation of a complex electric field can be estimated from the vector sum of a random complex vector to a complex electric field vector, where the relative length of the two vectors is determined by the SNR.<sup>21</sup> This can be translated into an angular standard deviation,  $\Delta\theta$ , in a Poincaré sphere representation of a measured polarization state such that  $\Delta\theta = \sqrt{2/\text{SNR}}$ . It should be noted that this relation takes into account amplitude variations between

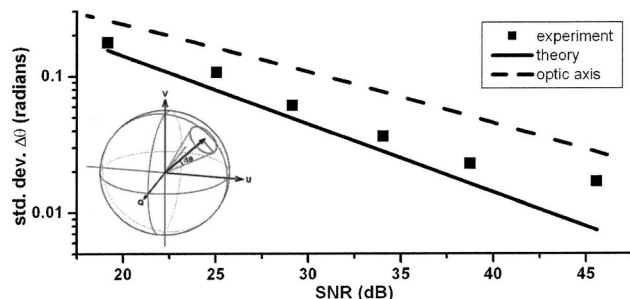


Fig. 2. Angular standard deviation in the Poincaré sphere,  $\Delta\theta$ , as a function of signal-to-noise ratio on a log-log scale for polarization state (squares, standard deviation over 1024 measurements; solid line, theoretical curve, see text) and optic axis determination (dashed line, simulated prediction, see text). Inset, Poincaré sphere illustrating a probability distribution as indicated by a cone defined by the standard deviation,  $\Delta\theta$ .

orthogonal electric field components. The experimental results show good agreement with predicted theory, except at 45 dB, where the combined power of the sample and reference arms was outside of the shot-noise-limited range of the system. Clearly, this relation will affect the accuracy of any resulting sample polarization properties. To calculate the effect on optic axis determination accuracy, numerical simulations that included variation of the relative orientation between the incident states and the optic axis were performed for a range of SNR values. Figure 2 shows the resulting prediction of the mean angular standard deviations for optic axis determination as a function of SNR.

In conclusion, we have presented a generalized analysis of fiber-based PS-OCT and demonstrated that the measured optic axes of a sample can be rotated out of the QU-plane in a Poincaré sphere representation by the system optical fibers. The orientation of the optic axis can be recovered accurately except for an inherent ambiguity in offset and sign, meaning that in any fiber-based system reported to date, only the magnitude of a change in optic axis orientation can be determined. Finally, we have demonstrated a fundamental limit on the accuracy with which a polarization state can be determined as a function of SNR, which affects the calculation of any sample polarization properties such as cumulative and differential birefringence, diattenuation, and optic axis orientation.

Research grants from the National Institutes of Health (R01-RR019768 and R01-EY014975) and the

U.S. Department of Defense (F4 9620-01-10014) are gratefully acknowledged. B. H. Park's email address is hylepark@helix.mgh.harvard.edu.

## References

1. J. F. de Boer, T. E. Milner, M. J. C. van Gemert, and J. S. Nelson, *Opt. Lett.* **22**, 934 (1997).
2. J. F. de Boer, S. M. Srinivas, A. Malekafzali, Z. Chen, and J. S. Nelson, *Opt. Express* **3**, 212 (1998).
3. M. J. Everett, K. Schoenenberger, B. W. Colston, and L. B. Da Silva, *Opt. Lett.* **23**, 228 (1998).
4. J. F. de Boer, T. E. Milner, and J. S. Nelson, *Opt. Lett.* **24**, 300 (1999).
5. G. Yao and L. V. Wang, *Opt. Lett.* **24**, 537 (1999).
6. C. K. Hitzengerger, E. Gotzinger, M. Sticker, M. Pircher, and A. F. Fercher, *Opt. Express* **9**, 780 (2001).
7. J. F. de Boer and T. E. Milner, *J. Biomed. Opt.* **7**, 359 (2002).
8. C. E. Saxer, J. F. de Boer, B. H. Park, Y. H. Zhao, Z. P. Chen, and J. S. Nelson, *Opt. Lett.* **25**, 1355 (2000).
9. B. H. Park, M. C. Pierce, B. Cense, and J. F. de Boer, *Opt. Express* **11**, 782 (2003).
10. S. L. Jiao, G. Yao, and L. V. Wang, *Appl. Opt.* **39**, 6318 (2000).
11. S. L. Jiao and L. V. Wang, *J. Biomed. Opt.* **7**, 350 (2002).
12. S. L. Jiao and L. V. Wang, *Opt. Lett.* **27**, 101 (2002).
13. S. Jiao, W. Yu, G. Stoica, and L. V. Wang, *Opt. Lett.* **28**, 1206 (2003).
14. B. H. Park, M. C. Pierce, B. Cense, and J. F. de Boer, *Opt. Lett.* **29**, 2512 (2004).
15. B. Cense, H. C. Chen, B. H. Park, M. C. Pierce, and J. F. de Boer, *J. Biomed. Opt.* **9**, 121 (2004).
16. J. E. Roth, J. A. Kozak, S. Yazdanfar, A. M. Rollins, and J. A. Izatt, *Opt. Lett.* **26**, 1069 (2001).
17. J. Zhang, S. G. Guo, W. G. Jung, J. S. Nelson, and Z. P. Chen, *Opt. Express* **11**, 3262 (2003).
18. B. H. Park, C. Saxer, S. M. Srinivas, J. S. Nelson, and J. F. de Boer, *J. Biomed. Opt.* **6**, 474 (2001).
19. S. L. Jiao and L. V. Wang, *Opt. Lett.* **29**, 2875 (2004).
20. M. C. Pierce, B. H. Park, B. Cense, and J. F. de Boer, *Opt. Lett.* **27**, 1534 (2002).
21. B. H. Park, M. C. Pierce, B. Cense, M. Mujat, and J. F. de Boer, *Opt. Express* **13**, 3931 (2005).
22. B. Cense, T. C. Chen, B. H. Park, M. C. Pierce, and J. F. de Boer, *Opt. Lett.* **27**, 1610 (2002).
23. W. K. Tung, *Group Theory in Physics* (World Scientific, 1985).
24. B. H. Park, M. C. Pierce, and J. F. de Boer, *Opt. Lett.* **29**, 2873 (2004).
25. S. Yazdanfar, C. H. Yang, M. V. Sarunic, and J. A. Izatt, *Opt. Express* **13**, 410 (2005).